Journal of Zhejiang University-SCIENCE A (Applied Physics & Engineering)
ISSN 1673-565X (Print); ISSN 1862-1775 (Online)
www.zju.edu.cn/jzus; www.springerlink.com
E-mail: jzus@zju.edu.cn

Prediction of thermal fatigue life of a turbine nozzle guide vane*

Xin-qian ZHENG†[1], Tao DU[2], Yang-jun ZHANG[1]

([1]*State Key Laboratory of Automotive Safety and Energy, Tsinghua University, Beijing 100084, China*)

([2]*Beijing Power Machinery Research Institute, Beijing 100074, China*)

†E-mail: zhengxq@tsinghua.edu.cn

Received May. 19, 2010; Revision accepted Sept. 7, 2010; Crosschecked Jan. 25, 2011

Abstract: Thermal fatigue (TF) is one of the most important factors that influence turbine's life. This paper establishes a 3D solid-fluid coupling model for a steady temperature analysis of a high-pressure turbine nozzle at different turbine inlet gas total temperatures (TIGTTs). The temperature analysis supplies the temperature load for subsequent 3D finite element analysis to obtain the strain values. Following this, the prediction of the TF life is made on the basis of equivalent strain range. The results show that the strain increases with TIGTT, and the predicted TF life decreases correspondingly. This life prediction was confirmed by one TF test.

Key words: Engine, Nozzle guide vane, Thermal fatigue (TF) life, Solid-fluid
doi:10.1631/jzus.A1000233 **Document code:** A **CLC number:** V235.1

1 Introduction

Fatigue is one of the most important factors that influence the damage and the failure life for those components working under variable loads. About 80% of the failures for the engine components are due to various types of fatigue. Thermal fatigue (TF) is the main kind of failure for the engine components, especially for hot working parts.

TF phenomena were first discovered in electron beam collectors of high-power microwave devices. More recently, the demand for higher specific power has required higher operating temperature of an engine part, so TF analysis has become more and more important. For materials exhibiting cracks, many investigators have studied TF through crack growth (Musi and Beaud, 2003; Morita *et al*., 2004; Malesys *et al.*, 2008; Piehler and Damiani, 2008; Zhou and Yu, 2008; Asayama *et al*. 2009). Different methods have been developed for crack analysis. The probabilism combined with the finite element analysis (FEA) is widely applied. Asayama *et al*. (2009) developed a structural reliability evaluation method using probabilistic prediction of crack depth distributions for TF. This method is an extension of a probabilistic crack mechanics approach. It is capable of modeling crack initiation, crack propagation, and crack depth density distribution at a given cycle. Three dimensional finite element models (FEM) were constructed from the available test measurements, and used to obtain representative stress histories (Morita *et al*. 2004). The FEA stress results were used to perform fatigue usage and crack growth curves to determine the fatigue initiation and crack growth characteristics of the spacer ring cracks.

On the other hand, TF has been intensively investigated in experimental studies combined with the FEA. The FEA simulation allows better understanding of the evolution of the local stress-strain response. The results from thermal-structural FEA have been used to predict cycles of crack initiation in TF tests of some components (Akay *et al.*, 2003; Angelis and Palomba, 2004; Jones *et al.*, 2004; Mönig *et al.*, 2004; Sakhuja and Brevick, 2004; Angileri *et al*., 2006;

* Project (No. 50806040) supported by the National Natural Science Foundation of China

Wong and Chu, 2006; Chamani *et al.*, 2007; Damiani *et al*., 2007; Kaisaki *et al*., 2008; Bao *et al*., 2010). A thermal and structural 3D FEA has been conducted, and the results have been used to predict the fatigue crack initiation by strain-based fatigue-life algorithms (Damiani *et al.*, 2007). A detailed analysis was conducted on a centrifugal gray cast iron liner using different computer aided engineering tools to provide a more accurate estimate of thermo-mechanical loads (Chamani *et al.*, 2007).

A reliable and effective nozzle is the crucial component of a turbo-fan engine. For the improvement of engine efficiency, increasing the turbine inlet gas temperature is considered an available approach. However, it will result in a poor working environment and worse TF performance of the high-pressure turbine (HPT) nozzle guide vanes. Yet, conducting an experiment to assess TF life at various turbine inlet gas temperatures is too expensive to generalize. A low cost alternative is to simulate it with FEA technique. Sakhuja and Brevick (2004) predicted the number of copper rotor die-casting cycles to failure as a function of bulk die temperature for Haynes 230 and Inconel 617 alloys. To achieve these goals, a 2D thermo-mechanical FEA was performed to evaluate the strain ranges on selected die surfaces. Some empirical heat transfer coefficients and temperatures of some points were given as the boundary conditions for thermal analyses. Convection is one of the most important processes for heat transfer. In general, some experiential functions have been used to obtain the heat transfer coefficients. Thus, it is more applicable for a simple structure than a complex one.

In this study, for the complex structure of nozzle guide vanes, a better method is used to make a more accurate estimate of the temperature loads. This paper develops a 3D solid-fluid coupling model, with which a steady temperature analysis of an HPT nozzle is performed with a range of turbine inlet gas total temperature (TIGTT) (827−1327 °C). The TF life is revealed from the structural analysis by developing a 3D elasto-plastic FEA model, with the temperature loads coming from the aforementioned solid-fluid coupling model, rather than assuming some boundary temperatures and some heat transfer coefficients by experience. Based on the total strain ranges obtained from these analyses, the TF life of the HPT nozzle guide vane is predicted. The method of universal slopes (strain life method) is employed for the TF life predictions. To the author's knowledge, there is scarcely any study on the application of solid-fluid coupling model for the prediction of TF life. This numerical analysis process is suitable for all types of nozzle guide vanes.

2 Material properties

The nozzle guide vanes are made from nickel-base cast super-alloy K417, of which the pertinent temperature dependent physical and mechanical properties involved in the FEA are shown in Table 1. K417 alloy is suitable for high temperature applications, such as turbine blades and nozzle guide vanes, and it can resist high temperatures, up to 950 °C.

Table 1 Temperature dependent properties of K417

T (°C)	σ_b (MPa)	K (W/(m·K))	YS (MPa)	α ($\times10^{-6}$, K^{-1})	E (GPa)
700	966	20.52	781	14.2	171
800	888	22.61	744	14.7	165
900	669	24.28	454	15.5	156
1000	429	–	–	15.5	144

T: temperature; σ_b: ultimate tensile strength; K: thermal conductivity; YS: yield strength at 0.2% offset; α: thermal expansion coefficient; E: modulus of elasticity

3 Solid-fluid coupling analysis

The HPT guide is one of the parts in turbo-fan engines, which are exposed to high temperature and situated between a low pressure turbine guide and a combustion chamber. These vanes are hollow and cooled by internal cooling airflow.

As the basis for structural analysis, the steady temperature is simulated for the HPT guide vane with a solid-fluid coupling model. That is, a solid domain and two fluid domains are all included in simulation, and their temperature distributions are calculated at the same time. Considering the solid-fluid coupling, the interfaces between the solid domain and the fluid domains are taken as the inner boundary. A small change in fluid domain will affect temperature distribution directly. Consequently, the temperature values obtained through the solid-fluid coupling model will be more reliable than those through experiential heat transfer coefficients.

3.1 Numerical method

In this study, one solid subdomain and two fluid subdomains are included, and the heat transfer between them is automatically calculated. At the interface, the solver calculates both the fluid-side and solid-side temperatures based on the heat flux conservation.

Within the solid domain, the conservation of energy equation is simplified since there is no inside flow, and thus conduction is the only mode of heat transfer. The heat conduction through the solid without energy source has the following transport equation:

$$\frac{\partial}{\partial t}(\rho c_{\mathrm{p}} T) = \nabla \cdot (\lambda \Delta T). \tag{1}$$

Fluid domains are modeled as incompressible. The instantaneous equations of mass, momentum, and energy conservation can be written as follows in a stationary frame:

$$\frac{\partial \rho}{\partial t} + \nabla \cdot (\rho \vec{\boldsymbol{U}}) = 0, \tag{2}$$

$$\frac{\mathrm{d}(\rho \vec{\boldsymbol{U}})}{\mathrm{d}t} = \rho \vec{\boldsymbol{F}} - \Delta p + \mu \Delta \vec{\boldsymbol{U}}, \tag{3}$$

$$\frac{\mathrm{d}(\rho c_{\mathrm{p}} T)}{\mathrm{d}t} = \boldsymbol{\Phi} + \lambda \Delta T + \rho q, \tag{4}$$

where ρ, c_{p}, and λ are the density, specific heat capacity, and thermal conductivity of the solid or fluid, respectively. T is the temperature, t is the time, p is the pressure, $\vec{\boldsymbol{U}}$ is the vector of velocity, $\vec{\boldsymbol{F}}$ is the vector of force, μ is the dynamic viscosity, $\boldsymbol{\Phi}$ is the energy dissipation function, and q is the quantity of heat.

3.2 Analysis layout

The turbine nozzle is a symmetric cycle with 19 vanes. Therefore, instead of dealing with the whole structure, analysis of 1/19 of the structure yields complete results to reduce the numerical solution time; that is, the analysis model involves only one vane.

The domain of computation is divided into three subdomains, nozzle (A), cooling airflow (B), and gas (C) (Fig. 1). The subdomains of gas and cooling airflow are the fluid domains, and that of nozzle is the solid domain. The grids are generated within these subdomains. The grids near the boundaries are relatively dense and orthogonal to surface. The exclusive purpose of this solid-fluid coupling analysis is to obtain the temperature of the nozzle guide vane. Therefore, relatively coarse and reasonable meshing is applied in this analysis to save solution time.

The surface of the guide vane is taken for the coupling interaction between the fluid domain and the solid domain, through which the relationship of temperature between the vane and the gas or the cooling airflow is created.

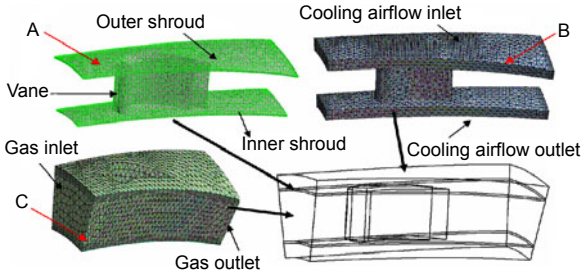

Fig. 1 Meshing for solid-fluid coupling analysis
A: nozzle; B: cooling airflow; C: gas

3.3 Boundary conditions

It is sure that the requirement for higher efficiencies of turbo-fan engines will lead to higher temperatures of turbine inlet gas. With the improvement of material performance and cooling technology, the temperature of turbine inlet gas has been raised to 1530−1720 °C from the initial 930−1030 °C (Lin, 2006). This creates the requirement of TF analysis with a wider range of temperature.

Entrance condition: the total pressures of the gas and cooling airflow are set to 140 and 130 kPa, respectively. The total temperature of the cooling airflow is set to 420 °C, based on the actual condition. The total temperature of the gas has an important impact on TF life, which is investigated as follows. Eight total temperatures are considered for analysis: 827, 927, 1027, 1127, 1177, 1227, 1277, and 1327 °C. The entrance flow directions are normal to the boundary conditions. The initial temperature of the nozzle guide vane is set to 25 °C.

Exit condition: the outlet static pressures of the gas and the cooling airflow are all given as 120 kPa. The exit flow directions are normal to the boundary conditions.

Wall condition: the speeds on the wall, the gradient of pressure, and the temperature in the normal direction are set to zero.

3.4 Simulation results

There are 12 representative points (labeled as points 1−12) that demonstrate the temperature, stress, and strain distributions of the nozzle guide vane (Fig. 2). The following nonlinear stress/strain analyses will also focus on these points. Points 1−4 are situated near the outer shroud (tip) and points 9−12 near the inner shroud (hub), while points 5−8 are situated on the central section of the vane. From another viewpoint, points 1, 5, and 9 are situated on the leading edge, and points 3, 7, and 11 on the trailing edge. Points 2, 6, and 10 are situated on the middle part of the basin surface, and points 4, 8, and 12 on the convex surface.

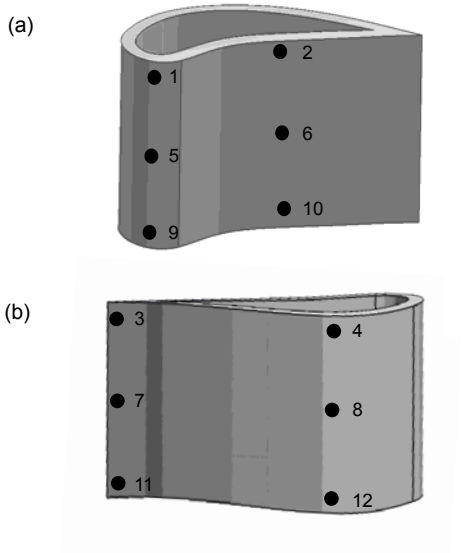

Fig. 2 Critical points locations on the vane
(a) Basin surface; (b) Convex surface

For the TIGTT of 1127 °C, the temperature distribution of the nozzle guide vane is shown in Fig. 3. It is an uneven temperature distribution with the lowest temperature observed at the central section of the vane basin with a value of 770 °C. Mostly, for the thick structure of trailing edge, the highest temperature is observed at the trailing edge near the outer shroud (tip) with a value of 930 °C. For the higher velocity of gas, the temperature of the vane convex surface is higher than that of the vane basin, with a value of about 820 °C.

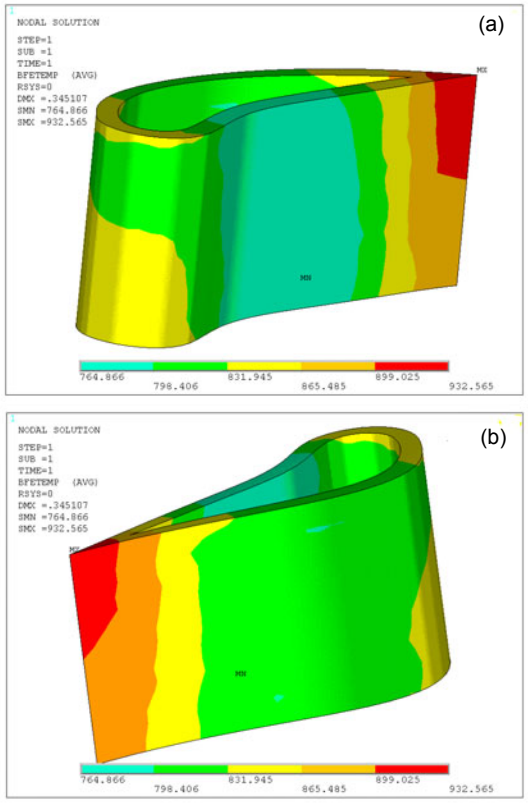

Fig. 3 Temperature distributions of the nozzle guide vane
(a) Basin surface; (b) Convex surface

Temperature of points 1−12 as a function of TIGTT is shown in Fig. 4, and excellent correlation between them is illustrated. It can be explicated that the temperature distributions of different TIGTTs are similar. The temperature of the trailing edge is higher than that of the leading edge due to the higher velocity of gas and thinner structure. On the other hand, the temperature of the convex surface is higher than that of the basin surface due to the higher velocity of gas. For the small thickness of vane, no obvious temperature gradient is found between the inner surface and the outer surface, although the inner surface is cooled by the internal cooling airflow.

4 Structural analyses

The temperature of the HPT nozzle changes quickly, and the temperature gradient is quite large after starting the engine. Furthermore, the guide vane is constrained by an outer shroud and an inner shroud. Thus, large thermal stress and strain appear, followed

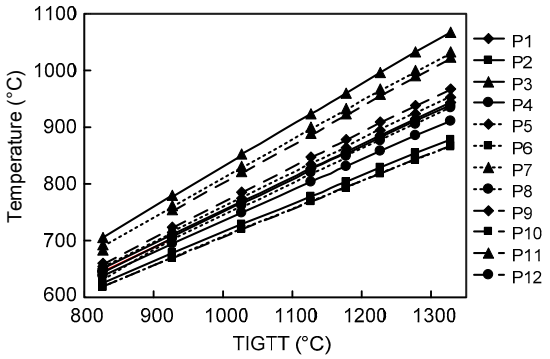

Fig. 4 Temperatures of points as a function of TIGTT

by TF. An engine works by starting and stopping as a cycle; that is, thermal stress and strain appear again and again. Thus, TF becomes significant, and TF failure can be considered as the major factor of reliability for guide vanes. As the basis of TF life prediction, an elasto-plastic structural analysis is performed here as a major part of this study.

4.1 Numerical method

During simulation, the material thermal properties vary with temperature. The stress-strain relations for an isotropic body are given by

$$\mathrm{d}\sigma=\boldsymbol{D}\mathrm{d}\varepsilon-\boldsymbol{C}\mathrm{d}T, \tag{5}$$

where $\mathrm{d}\sigma$ is the stress increment, $\boldsymbol{D}$ is the elastic matrix for elastic region or elasto-plastic matrix for plastic region, $\boldsymbol{C}$ is the matrix related to temperature and thermal expansion coefficient, $\mathrm{d}T$ is the temperature increment, and $\mathrm{d}\varepsilon$ is the total strain increment, which can be given as

$$\mathrm{d}\varepsilon=\mathrm{d}\varepsilon_\mathrm{p}+\mathrm{d}\varepsilon_\mathrm{e}+\mathrm{d}\varepsilon_\mathrm{T}, \tag{6}$$

where $\mathrm{d}\varepsilon_\mathrm{p}$ is the plastic strain increment, $\mathrm{d}\varepsilon_\mathrm{e}$ is the elastic strain increment, and $\mathrm{d}\varepsilon_\mathrm{T}$ is the thermal strain increment. The kind of elasto-plastic hardening law is kinematic hardening.

4.2 Boundary conditions and loads

The nozzle guide is a stationary component subjected to aerodynamic force and temperature loads. It is suggested that the influence of aerodynamic force on TF failure is negligible compared to the high temperature loads acting on the vane surfaces. Therefore, it is not included in the simulation. On the basis of the aforementioned solid-fluid coupling analysis, temperature loads are applied to the nozzle guide vane.

The installation sketch of the HPT nozzle is shown in Fig. 5. There are two flanges on the outer shroud. The rear flange surface (A-A) is fixed to low-pressure turbine nozzle, and the front flange surface (B-B) is fixed to the combustion chamber.

The following boundary conditions and loads are applied for the structural analysis: (1) temperature loads come from foregoing solid-fluid analysis; and (2) those nodes attached to each side of the outer shroud of the nozzle (A-A and B-B sections as shown in Fig. 5) are constrained, and the displacements along the radial and axial directions are set to zero.

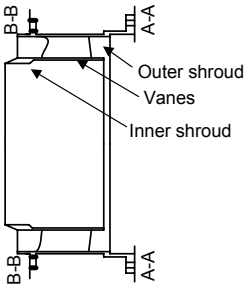

Fig. 5 Sketch of the HPT nozzle

4.3 Finite element model

The object of the structural analysis is a nozzle guide vane, i.e., the solid domain in foregoing solid-fluid analysis. The model is rebuilt for refined FEA meshing containing about 13 000 elements. A type of isoparametric hexahedron solid element is employed. Thermal stress and strain are elasto-plastically calculated by FEA. The model for analysis and the boundary conditions are shown in Fig. 6.

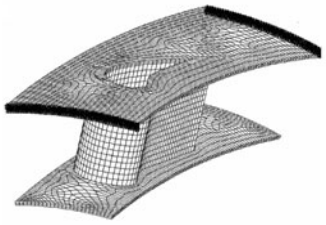

Fig. 6 Finite element analysis model

4.4 Simulation results

This section discusses the post-processing results from analysis. The strain values obtained here

are taken for the basis of TF life prediction. To evaluate the number of cycles to failure for a given situation, an appropriate strain component should be used. In this case, for the multiaxial stress state, the von Mises equivalent strain range is considered in fatigue life evaluation (Sakhuja and Brevick, 2004). TF does not correspond to a uniaxial stress state, but hydrostatic stress effect is not considered in our case, because it is in very low cycle fatigue regime.

The von Mises equivalent strain and stress are defined as

$$\varepsilon_{\mathrm{eq}}=\sqrt{\bar{\varepsilon}^2+\gamma^2/3},\ \sigma_{\mathrm{eq}}=\sqrt{\sigma^2+3\tau^2}, \tag{7}$$

where $\bar{\varepsilon}=2(1+\nu)/3\varepsilon^{\mathrm{e}}+\varepsilon^{\mathrm{p}}$, ε^{e} and ε^{p} are the elastic and plastic axial strains, respectively, ν is the Poisson's ratio, and γ is the torsional strain. σ and τ are the axial stress and torsional stress, respectively.

In this simulation, the von Mises stress and total strain are obtained at different TIGTTs. As an example, the von Mises equivalent strain and stress of the nozzle guide vane at a TIGTT of 1127 °C are shown in Fig. 7. The equivalent strains will be applied for the following life prediction.

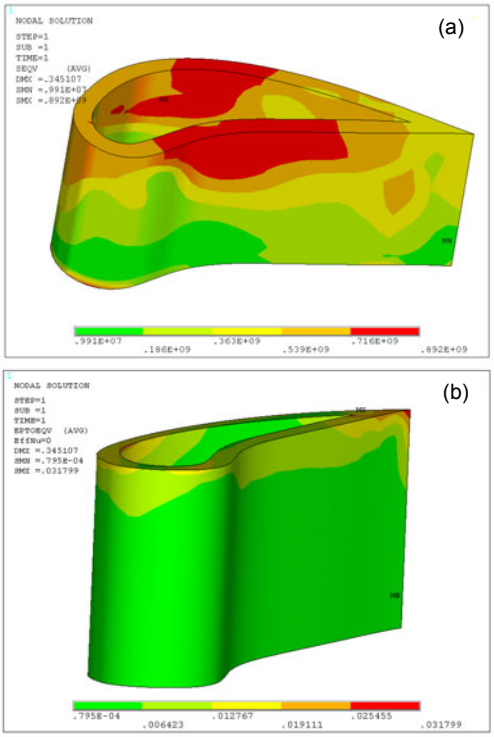

Fig. 7 von Mises equivalent stress (a) and strain (b) of the nozzle guide vane

The von Mises equivalent stress versus TIGTT at points 1−12 is shown in Fig. 8. The relationship between the equivalent strain and TIGTT is shown in Fig. 9.

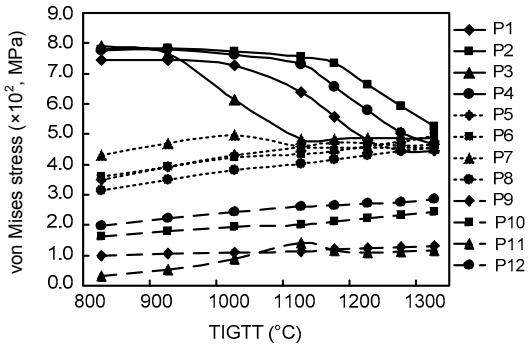

Fig. 8 Relationship between the von Mises stress and TIGTT

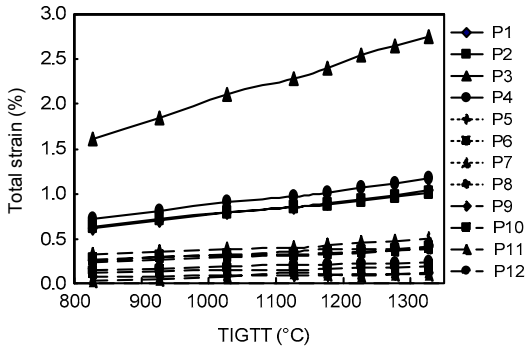

Fig. 9 Relationship between the total strain and TIGTT

From Fig. 8, it can be seen that some of the von Mises equivalent stress is decreased at high TIGTTs due to the decrease of yielding strength at high temperatures. As shown in Fig. 9, larger strains can be observed at points 1−4. These points are all near the outer shroud for two reasons, the high temperature gradient between nozzle guide vane and outer shroud, and the restriction on each side of the outer shroud. Furthermore, it can be seen that strains at these points increase with the TIGTT. At point 3, the highest strain appears (located on the trailing edge near the outer shroud).

5 Prediction of thermal fatigue life

TF is the main kind of failure for a nozzle guide vane. It is generated when the nozzle guide vane is heated and cooled repeatedly during starting and

stopping of engine, resulting in high thermal stress and TF crack on the surface of the nozzle guide vane. The high temperature low cycle fatigue (HTLCF) and TF have similar characteristics, because they both have the features of low cycle strain fatigue, and they are both subjected to high temperatures. The major difference is that the temperature of HTLCF remains constant, whereas the temperature of TF varies with stress. Except for the temperature and loads applied to the structure, the HTLCF and TF exhibit the same phenomena. At the same time, HTLCF is simpler, and has been studied more extensively. Thus, investigations of TF can be carried out through HTLCF (Ping and Guo, 1984).

If the temperature of HTLCF is taken as the equivalent temperature of TF, it can be assumed that life to failure of the TF would be the same as the HTLCF with the same strain range; i.e., they have the same $\Delta\varepsilon$-N_f curves, where $\Delta\varepsilon_e$ is the strain range, and N_f is the fatigue life. Considerable researches have been carried out (Ping and Guo, 1984; Goswami, 1997). The researches indicated that the equivalent temperature of TF varies with the material performance, temperature cycle, environment, etc. In general, if the plastic strain dominates, the average temperature of HTLCF temperature cycle would be taken as the equivalent temperature of TF. Contrarily, if the elastic strain dominates, the highest temperature of the HTLCF temperature cycle would be used.

For this work, the highest total strain is observed at point 3 with a conjecturable minimum predicted TF life. That is, this node is decisive for the life prediction for the guide vane. It can be seen obviously from the aforementioned analysis that the plastic strain of this node dominates. Therefore, the average temperature during thermal cycles should be taken as the equivalent temperature of TF.

The equations to predict the life of TF are derived by Manson (1966) as

$$\Delta\varepsilon_e = 3.5\frac{\sigma_b}{E}N_f^k, \tag{8}$$

$$\Delta\varepsilon_p = H^{0.6}N_f^c, \tag{9}$$

where $\Delta\varepsilon_e$ is the elastic strain range, $\Delta\varepsilon_p$ is the plastic strain range, and H is the logarithmic ductility. It is further stated that in Eqs. (8) and (9), these are material dependent constants. When Eqs. (8) and (9) are plotted on a log-log scale, straight curves appear, and constants k and c are the slopes of the curves.

Lacking of fatigue performance of K417 alloy, there is only one HTLCF $\Delta\varepsilon$-N_f curve at 900 °C available (Fig. 10).

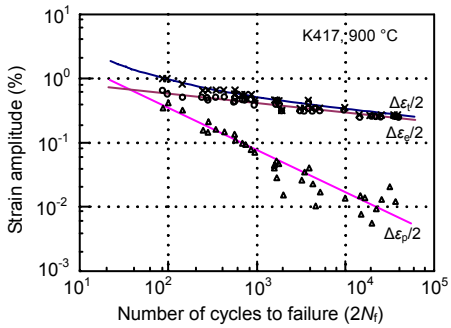

Fig. 10 $\Delta\varepsilon$-N_f curves of K417 alloy

Employing Eqs. (8) and (9), we arrive at the following formulae, which are used to describe functions between $\Delta\varepsilon_p$, $\Delta\varepsilon_e$, and N_f for K417 alloy:

$$\log\Delta\varepsilon_e = A + k\log N_f, \tag{10}$$

$$\log\Delta\varepsilon_p = 0.6\log H + c\log N_f, \tag{11}$$

where A is an assumed parameter. A, k, c, and H could be determined by Fig. 10, and A=−1.655, k=−0.166, c=−0.667, H=−0.01755.

By considering the mean stress and introducing the values of A, k, c, and H into Eqs. (8) and (9), the TF life of the nozzle guide vane can be estimated as

$$\begin{aligned}\Delta\varepsilon_t &= \Delta\varepsilon_p + \Delta\varepsilon_e \\ &= H^{0.6}N_f^c + 3.5\frac{\sigma_b - \sigma_m}{E}N_f^k \\ &= 0.0884N_f^{-0.667} + 0.022\left(1 - \frac{\sigma_m}{\sigma_b}\right)N_f^{-0.166},\end{aligned} \tag{12}$$

where $\Delta\varepsilon_t$ is the strain range, and σ_m is the mean stress. Depending on the definition of the TF life shown in Eq. (12), respective lives at different TIGTTs could be predicted. The strains of points 1−4 are obviously larger than those of other points; that is, these points are decisive for the TF of the vane. Thus, the strain range and the corresponding TF lives of these points are calculated, as shown in Table 2 and Fig. 11.

Table 2 Strain range and number of cycles to failure at points of interest

Point number	Strain range, $\Delta\varepsilon$ (%)							
	TIGTT (°C)							
	827	927	1027	1127	1177	1227	1277	1327
1	0.62	0.70	0.78	0.85	0.89	0.94	0.99	1.04
2	0.63	0.71	0.79	0.84	0.88	0.92	0.97	1.01
3	1.61	1.85	2.11	2.29	2.41	2.54	2.65	2.75
4	0.72	0.81	0.90	0.97	1.01	1.06	1.12	1.17
Point number	Number of cycles to failure, N_f							
	TIGTT (°C)							
	827	927	1027	1127	1177	1227	1277	1327
1	508	330	214	199	143	147	81	72
2	447	294	192	163	99	102	55	60
3	32	24	19	18	15	13	10	9
4	289	195	133	115	82	84	51	51

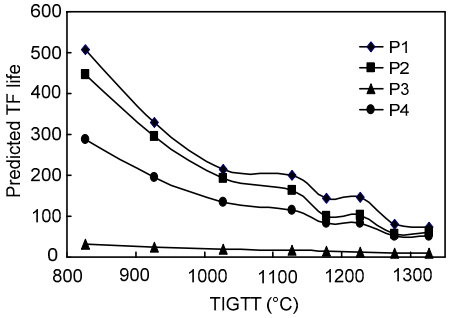

Fig. 11 Relationship between the predicted thermal fatigue life and TIGTT

As shown in Fig. 11, among the four points, point 3 has the worst TF performance with a corresponding shortest TF life. For the TIGTT of 1127 °C, the TF life of point 3 is predicted to be 18 cycles.

The predicted TF lives of these points are detected to decrease with TIGTT. It is known that the temperature of gas would affect the TF life severely. Thus, it is prerequisite to limit the raise of temperature for developing high efficiency engines.

6 Thermal fatigue tests

Experimentation has been performed on the HPT nozzle guide to confirm the numerical analysis. According to the reality, HPT nozzle guide was fixed in each side of the outer shroud. At the same time, the HPT nozzle guide was subjected to TF cycles induced by hot airflow. During a test cycle, hot airflow was present for 100 s, during which steady temperature was maintained, followed by natural cooling for 10 min. The total temperature of hot airflow was set to 1127 °C with a total pressure of 140 kPa during the tests. After testing for 23 cycles, TF cracks were observed at some nozzle guide vanes. Most cracks were located on the trailing edge near the outer shroud. The results are close to the prediction of the TF.

The zone of cracks was charcoal gray and covered with some oxide. It means that these cracks were formed at high temperatures. These cracks developed outside-in and propagated along the crystal grain boundary, which is one of the main characteristics of TF cracks. On the basis of the above analysis about these cracks, it can be seen that these cracks were induced by TF.

7 Conclusions

This paper has presented an overview of the TF life prediction for the nozzle guide vane. Based on the above analysis, the temperature of the HPT guide vane increases linearly with TIGTT. At the same time, stress and strain also increase with TIGTT. The larger strains are observed at those points near the outer shroud (tip). It also can be seen that predicted TF life of the HPT guide vane decreases severely with TIGTT.

The equivalent strain of point 3 is observed to be the highest, leading to the worst TF performance with the predicted TF life of 18 cycles when TIGTT is equal to 1127 °C. This point is located on the trailing

edge near the outer shroud (tip). The result indicates excellent correlation between the predicted (18 cycles) and the experimental TF life (23 cycles). The proposed numerical approach is able to satisfactorily predict the TF life of some hot parts of engines. Application of the numerical approach can reduce the economic cost and shorten the period for new developed engines.

Acknowledgements

The authors are deeply grateful to Hui-hua QIAN from Beijing Power Machinery Research Institute for her efforts to make the simulation possible. The author Xin-qian ZHENG would also like to thank Joern HUENTELER from RWTH Aachen University for his assistance with the English grammar.

References

Akay, H.U., Liu, Y., Rassaian, M., 2003. Simplification of finite element models for thermal fatigue life prediction of PBGA packages. *Journal of Electronic Packaging*, **125**(3):347-353. [doi:10.1115/1.1569956]

Angelis, G. D., Palomba, F., 2004. The Reliability Improvement of a Conventional Cast Iron Exhaust Manifold for a Small Size Gasoline Engine. ASME Internal Combustion Engine Division Fall Technical Conference Long Beach, California, USA.

Angileri, V., Bonavolontà, R., Durando, M., Garganese, M., Mariotti, G.V., 2006. FE Calculation Methodology for the Thermodynamic Fatigue Analysis of an Engine Component. ASME 8th Biennial Conference on Engineering Systems Design and Analysis Torino, Italy.

Asayama, T., Takasho, H., Kato, T., 2009. Probabilistic prediction of crack depth distributions observed in structures subjected to thermal fatigue. *Journal of Pressure Vessel Technology*, **131**(1):011402. [doi:10.1115/1.3027457]

Bao, S., Jin, W., Guralnick, S.A., Erber, T., 2010. Two-parameter characterization of low cycle, hysteretic fatigue data. *Journal of Zhejiang University-SCIENCE A (Applied Physics & Engineering)*, **11**(6):449-454. [doi:10.1631/jzus.A0900763]

Chamani, H., Shahangian, S.N., Jazayeri, S.A., 2007. Thermo-Mechanical Fatigue Life Prediction of a Heavy Duty Diesel Engine Liner. ASME Internal Combustion Engine Division Fall Technical Conference, Charleston, South Carolina, USA.

Damiani, T.M., Holliday, J.E., Zechmeister, M.J., Reinheimer, R.D., Jones, D.P., 2007. Thermal Fatigue Testing and Analysis of a Thick Perforated Ring. ASME Pressure Vessels and Piping Conference, San Antonio, Texas, USA.

Goswami, T., 1997. Low cycle fatigue life prediction-a new model. *International Journal of Fatigue*, **19**(2):109-115. [doi:10.1016/S0142-1123(96)00065-5]

Jones, D.P., Holliday, J.E., Leax, T.R., Gordon, J.L., 2004. Analysis of a Thermal Fatigue Test of a Stepped Pipe. ASME/JSME Pressure Vessels and Piping Conference, San Diego, California, USA.

Kaisaki, N., Takasho, H., Kobayashi, S., 2008. Spectra Thermal Fatigue Tests under Frequency Controlled Fluid Temperature Variation: Superposed Sinusoidal Temperature Fluctuation Tests. ASME Pressure Vessels and Piping Conference, Chicago, Illinois, USA.

Lin, Z.M., 2006. Manufacture status and develop direction of engines. *Journal of Aeroengine*, **32**(1):1-8.

Manson, S.S., 1966. Thermal Stress and Low Cycle Fatigue. McGraw-Hill, New York.

Malesys, N., Vincent, L., Hild, F., 2008. Probabilistic Modeling of Crack Networks in Thermal Fatigue. ASME Pressure Vessels and Piping Conference, Chicago, Illinois, USA.

Mönig, R., Keller, R.R., Volkert, C.A., 2004. Thermal fatigue testing of thin metal films. *Review of Scientific Instruments*, **75**(11):4997-5004. [doi:10.1063/1.1809260]

Morita, A., Kagawa, H., Kubo, S., 2004. Evaluation of Multiple Crack Propagation Behavior in a Gas Turbine Blade Under Thermal Fatigue Condition. ASME/JSME Pressure Vessels and Piping Conference, San Diego, California, USA.

Musi, S., Beaud, F., 2003. An Analytical Model for Thermal Fatigue Crack Initiation and Propagation in Mixing Zones of Piping Systems. ASME Pressure Vessels and Piping Conference, Cleveland, Ohio, USA.

Piehler, R.S., Damiani, T.M., 2008. Fatigue and Crack Growth Analysis of a Thick Instrumentation Ring Subjected to Thermal Fatigue Cycling. ASME Pressure Vessels and Piping Conference, Chicago, Illinois, USA.

Ping, X., Guo, Y.W., 1984. Thermal Stress and Thermal Fatigue. National defense industry Press, Beijing, China.

Sakhuja, A., Brevick, J.R., 2004. Prediction of thermal fatigue in tooling for die-casting copper via finite element analysis. *AIP Conferences Proceedings*, **712**(1):1881-1886. [doi:10.1063/1.1766807]

Wong, T.E., Chu, C., 2006. Thermal Fatigue Life Prediction Model of CCGA Tin-Lead and Lead-Free Interconnects. ASME International Mechanical Engineering Congress and Exposition, Chicago, Illinois, USA.

Zhou, X., Yu, X.L., 2008. Fatigue crack growth rate test using a frequency sweep method. *Journal of Zhejiang University-SCIENCE A*, **9**(3):346-350. [doi:10.1631/jzus.A0720009]